



**RESEARCH ARTICLE**

## **Geodetically Referenced Single-Beam Bathymetry of Erelu Reservoir, Nigeria for Sedimentation Assessment and Monitoring**

**Shittu, I.O.<sup>1\*</sup>, Hamid-Mosaku, I.A.<sup>2</sup>, Jimoh, O.A.<sup>2</sup>, Qaadri, J.A.<sup>1</sup>, Afonja, Y.O.<sup>1</sup>, Akindiya, O.M.<sup>1</sup>, Effiong, O.A.<sup>1</sup>**

<sup>1</sup>Department of Surveying and Geoinformatics, Federal School of Surveying, Oyo State, Nigeria.

<sup>2</sup>Department of Surveying and Geoinformatics, University of Lagos, Lagos State, Nigeria.

Corresponding email: [oyekesinro@gmail.com](mailto:oyekesinro@gmail.com) ; <https://orcid.org/0000-0002-7492-6987>

### **Abstract**

*Reservoir sedimentation threatens long-term storage capacity and operational reliability, particularly in developing regions where high-resolution hydroacoustic systems are unavailable. This study applies a geodetically referenced single-beam workflow to derive a benchmark-controlled bathymetric baseline for the Erelu Reservoir, Nigeria. A South SDE-28S+ EchoSounder integrated with GNSS and precise levelling was deployed along a structured grid, and depth measurements were converted to riverbed elevations using orthometric heights transferred from temporary benchmarks established for this survey. A zoned water-surface correction strategy was implemented to reduce vertical uncertainty and improve elevation fidelity in shallow, vegetation-obstructed areas. The reservoir exhibited depths ranging from 0.60 m to 6.00 m, revealing measurable spatial variation in riverbed elevation and the theoretical sensitivity of storage-volume estimates to small vertical offsets in benchmark-referenced bed geometry. The workflow offers a cost-effective solution for sedimentation monitoring in reservoirs lacking historical digital elevation models or construction records. Future work should integrate sediment cores, dual-frequency echogram interpretation, and uncertainty modelling to support material classification and sedimentation-rate estimation.*

### **ARTICLE HISTORY**

Received: 27<sup>th</sup> October, 2025

Accepted: 28<sup>th</sup> December, 2025

Published: 30<sup>th</sup> December, 2025

### **KEYWORDS**

Sedimentation  
Hydroacoustic Systems  
Single-Beam Sonar  
Riverbed Elevation  
Echogram Interpretation.

**Citation:** Shittu, I.O., Hamid-Mosaku, I.A., Jimoh, O.A., Qaadri, J.A., Afonja, Y.O., Akindiya, O.M., Effiong, O.A. (2025). Geodetically Referenced Single-Beam Bathymetry of Erelu Reservoir, Nigeria for Sedimentation Assessment and Monitoring, *Journal of Geomatics and Environmental Research*, 8(2). Pp205-217

### **1. INTRODUCTION**

Globally, sediment deposition in water bodies is a natural and ongoing geomorphic process resulting from the accumulation of transported particles (Springs, 2008). Over time, this process can reduce reservoir storage capacity, degrade water quality, and impair water availability for agricultural, industrial, and domestic use. Monitoring sediment accumulation is thus essential for sustaining the operational performance and longevity of reservoirs.

A wide array of techniques has been employed to monitor sedimentation in reservoirs, demonstrating their effectiveness across different environments. These include bathymetric surveys (Adediji, 2005; Ortt *et al.*, 2008; Springs, 2008; Ceylan *et al.*, 2011; Patil & Shektar, 2015; Chukwu and Badejo, 2015; Ajith, 2016; Adongo *et al.*, 2019; Shiferaw and Abebe, 2021; Moningkey *et al.*, 2022; Mekonnen *et al.*, 2022; Essel-Yorke, 2023), remote sensing and GIS-based approaches (Dadoria *et al.*, 2017; Mostofi *et al.*, 2019; Singh

*et al.*, 2023), combined bathymetric and remote sensing studies (Darama *et al.*, 2019; Lopes and de Araújo, 2019; Güvel *et al.*, 2021; Iqlash, 2025), and various analytical approaches (Patil and Shetkar, 2016).

A common shortfall in many sedimentation studies, particularly those using single-beam systems, is the reliance on volumetric comparisons without rigorous consideration of water-surface elevation and the relative elevation of the reservoir bed to a known geodetic benchmark. For example, although studies such as Mekonnen *et al.* (2022) and Shiferaw and Abebe (2021) convert depth measurements into elevations, they often rely on assumed or instrument-derived water surface levels without referencing a fixed geodetic benchmark, which may introduce vertical uncertainty. This is particularly problematic in shallow reservoirs, where even small elevation errors can lead to significant miscalculations in sediment volume.

Despite their limited ability to discriminate sediment layers, single-frequency single-beam Echosounders remain a reliable tool for generating baseline bathymetric surfaces when paired with accurate positional and elevation referencing. Establishing such a geodetically controlled baseline is vital in reservoirs lacking historical Digital Elevation Models (DEMs) or original design records.

Accordingly, the objective of this study is to develop a standards-compliant, GNSS-integrated single-beam method tailored for resource-limited, shallow, or newly impounded reservoirs. The approach emphasizes precise levelling from known benchmarks and conversion of depth data to reservoir bed elevations. The waterbody is divided into spatial zones, each assigned an average water surface level (WSL) to improve the accuracy of depth-to-elevation conversion.

The Erelu Reservoir in southwestern Nigeria served as the pilot site for the application of this methodology. Temporary control points were established along the reservoir banks, and orthometric heights were transferred to the water surface using precise levelling techniques, ensuring high positional fidelity across all measurements. By subdividing the reservoir into hydrologically consistent zones and assigning localized WSL values, vertical uncertainty in the bathymetric model was minimized, establishing a reliable baseline for future sedimentation monitoring and water resource planning.

While single-beam Echosounders are widely used for bathymetric mapping, existing literature rarely evaluates their accuracy under shallow, vegetation-dominated reservoir conditions or applies geodetic water-level referencing to minimize vertical bias. Previous studies either assume fixed water levels or rely on Echosounder-derived elevations that are not referenced to a geodetic benchmark, potentially introducing systematic vertical errors exceeding the magnitude of annual sedimentation. This gap is particularly critical in reservoirs lacking historical reference elevations, where establishing a repeatable baseline is essential. This study addresses this limitation by testing whether zone-based water-level corrections improve spatial accuracy relative to a uniform correction approach, providing a methodological improvement over previous single-beam sediment studies in Nigeria and broader Africa.

## 2. STUDY AREA

The Erelu Reservoir, located in Oyo Town in southwestern Nigeria, lies north of Ibadan. Geographically, it is positioned between latitudes 7°53' and 7°55'N and longitudes 3°53' and 3°56'E. Constructed in 1961 by the former Western Region government on the Awon River, the reservoir is fed by several tributaries, including Isuwin, Orok, Ogbagba, Oloro, Elesin, and Abata, primarily to supply potable water to the surrounding communities. It also serves as an important nursery and breeding ground for a wide variety of fish species, supporting extensive fishing activities in the area. The catchment area is estimated to range between 243.36 km<sup>2</sup> and 315.86 km<sup>2</sup>, while the impoundment area is approximately 161.07 hectares. As of January 2023, the maximum recorded depth of the reservoir was 5.89 meters, increasing to 6.00 meters by August 2023, with a corresponding riverbed reduced level of 233.14 meters. The region experiences distinct dry and rainy seasons, with an average temperature of 27°C, annual rainfall of approximately 591.6 mm, and a mean annual relative humidity of 77.16%. The reservoir is surrounded by evergreen vegetation interspersed with grasses, and its banks support aquatic and semi-aquatic plants such as *Pistia stratiotes*, *Commelinaceae*, and *Ipomoea aquatica*. The area also hosts settlers from various Nigerian states, including Oyo, Ogun, Ondo, Kogi, Benue, and Delta, contributing to a diverse socio-economic environment in the region (Shittu *et al.*, 2024; Olasunkanmi *et al.*, 2021; Popoola *et al.*, 2019; Kareem *et al.*, 2018; Kareem *et al.*, 2016; Falaye *et al.*, 2015; Ufoegbuna *et al.*, 2011).

The surveyed area (Figure 1) spans Easting 598000mE – 601000mE and Northing 871000mN – 874000mN, referenced to WGS 1984 / UTM Zone 31N. The surveyed portion is indicated in blue, while the unsurveyed portion, located less than 1 km from the Awon River, and is shown in red due to obstruction by dense aquatic vegetation. As such, the dataset should be regarded as a baseline for future sedimentation assessment, noting that data collection occurred during the rainy season.

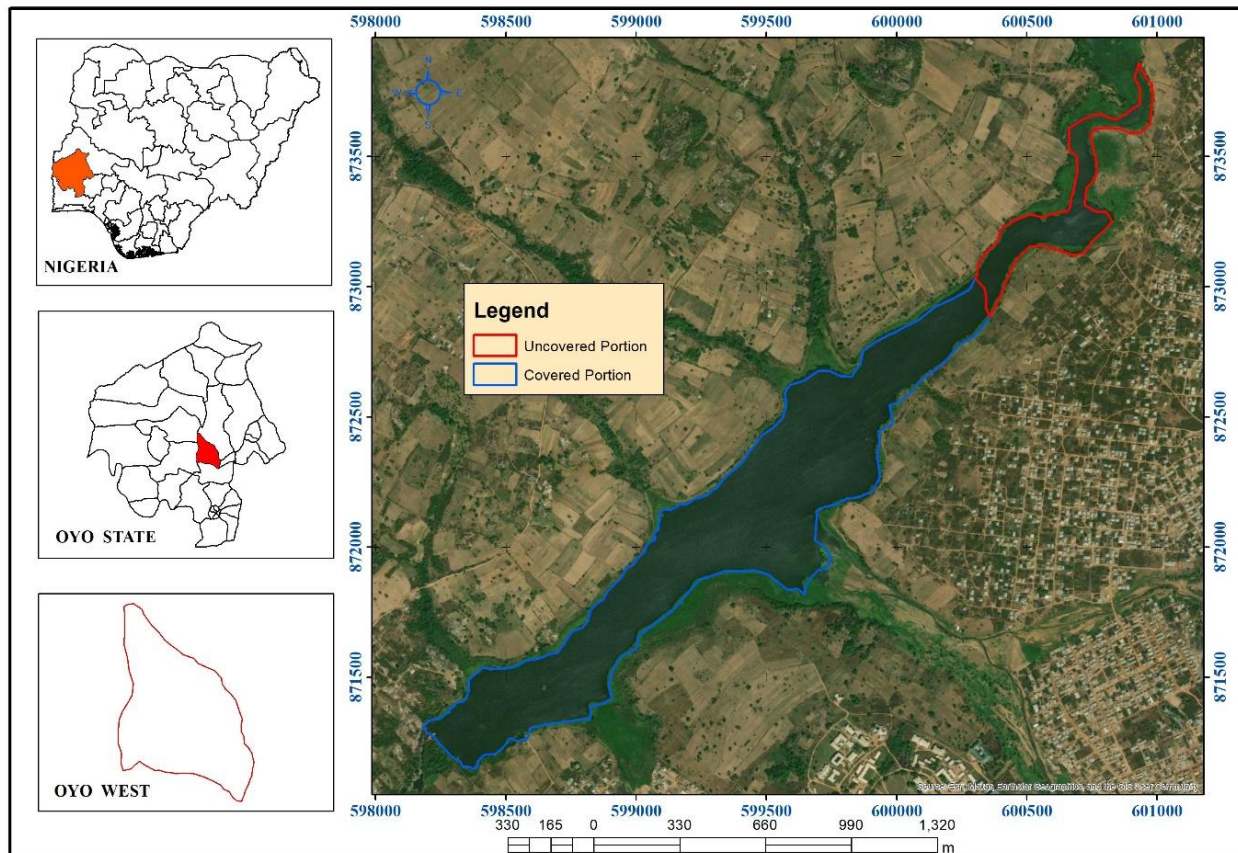


Figure 1. Surveyed (Blue) and Unsurveyed (Red) areas of Erelu Reservoir (Source: Researchers, August 2023).

### 3. DATA SOURCE, COLLECTION AND PROCESSING

A South SDE-28S+ single-beam EchoSounder operating at 200 kHz with a 7° beam angle was used to acquire depth measurements. The system records depths with a resolution of 0.01 m and an accuracy of  $\pm 1 \text{ cm} \pm 0.1\%$  of depth. Depth measurements were logged at an average ping rate of 14 Hz, with automatic gain control (AGC) and time-varied gain (TVG) applied during acquisition. The instrument supports a depth range of 0.3–300 m, and sound velocity was configured between 1300–1700 m/s range based on field conditions. Draft correction was applied during post-processing.

Positional data were acquired using a multi-constellation GNSS receiver capable of tracking GPS, GLONASS, Galileo, BeiDou, and SBAS signals. The receiver operated at a logging rate of 1 Hz and output data in standard NMEA-0183 format. Under standalone conditions, the GNSS typically provides horizontal accuracy of a few metres, while centimetre-level precision is achievable with differential or RTK corrections. All coordinates were referenced to the WGS 1984 datum, UTM Zone 31N. Established protocols outlined by Shittu *et al.* (2024), the Surveyors' Council of Nigeria (SURCON), and the International Hydrographic Organization (IHO) were rigorously followed throughout the process.

The survey focused on navigable sections of the reservoir free of aquatic weeds and rocky obstructions to ensure consistent acoustic returns. Depth measurements were then combined with water-surface reduced levels (RLs) derived from benchmarks. Relative water-surface heights were determined by transferring

orthometric heights from temporary benchmarks to the water surface through precise levelling at selected locations. Benchmarks were positioned on stable ground above the high-water line and away from sandy or erosion-prone banks to ensure long-term stability.

Using Equation 1, the orthometric heights of the temporary benchmarks (Table 1), along with staff readings and water-surface observations along the reservoir boundary (Figure 2), were used to calculate the reduced levels (RLs) of the water surface. These RLs were combined with the depth measurements to derive riverbed elevations. To account for spatial variability in water levels, the reservoir boundary was subdivided into hydrologically consistent zones (Table 2), and an Average Reduced Water-Surface Level (ARLWS) was calculated for each zone using Equation 2. This zonal approach ensures that elevation referencing does not rely on a single water-surface value for the entire reservoir.

$$RL_{WS} = RL_{TBM} + BS_{TBM} - FS_{WS} \quad (1)$$

$RL_{WS}$  = Reduced level of the water surface

$RL_{TBM}$  = Reduced level of the temporary benchmark

$BS_{TBM}$  = Backsight reading on the benchmark

$FS_{WS}$  = Foresight reading on the water surface

Table 1. Benchmark Coordinates and Reduced Water Levels

Benchmark Information (in meters)					Levelling Data (m)			Reduced Level (m)	
Zone	ID	Easting	Northing	Elevation	$BS_{TBM}$	$IS_{TBM}$	$FS_{WS}$	$RL_{WS}$	Remarks
1	TBM 01	598627.635	871276.291	240.883	0.773	2.769	2.735	238.921	WSH 01
								238.887	TP 01
2	TBM 02	598698.778	871299.187	240.537	0.827		2.135	239.229	WSH 02
	TBM 03	598527.460	871573.767	240.317	0.787		1.835	239.269	WSH 03
	TBM 04	599472.363	871783.221	240.601	1.623		1.465	240.759	WSH 04
	TBM 05	599608.530	871752.528	240.758	0.209		1.629	239.338	WSH 05
	TBM 06	599325.108	872282.343	240.261	1.126		2.159	239.228	WSH 06
	TBM 07	599444.820	872401.913	240.620	1.677		2.345	239.952	WSH 07
3	TBM 08	600246.774	872760.370	241.064	0.765		2.228	239.601	WSH 08
	TBM 09	600327.510	872812.065	241.165	0.518		1.965	239.718	WSH 09

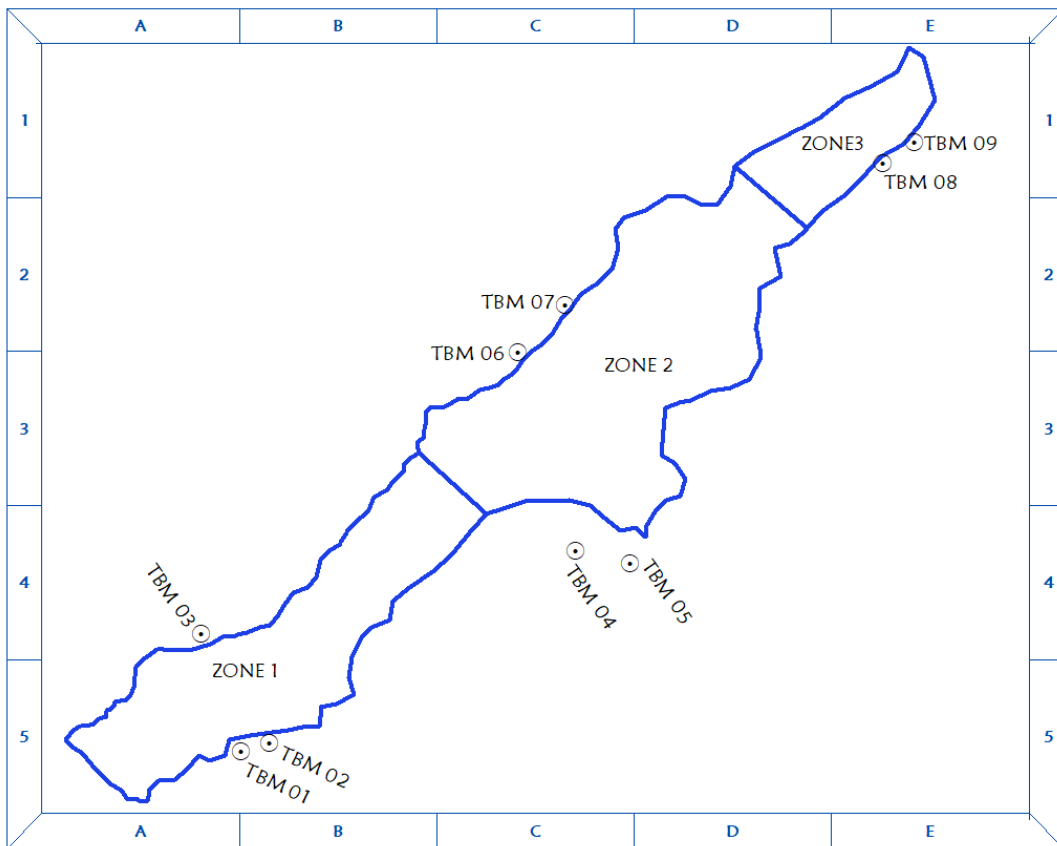


Figure 2. Reservoir boundary with zoning divisions and water-surface observation points

$$ARLWS_i = \frac{1}{n_i} \sum_{k=1}^{n_i} RL_{WS,k} \quad (2)$$

$i$  = zone number

$k$  = measurement index *within* zone  $i$

$n_i$  = number of water-surface measurements in zone  $i$

$RL_{WS,k}$  = reduced level of the water surface at measurement  $k$

Table 2. Divisions into zones

Zone	Water Surface ID	Reduced Level (m)	Average Reduced Level (m)
1	WSH 01	238.921	
	WSH 02	239.229	239.140
	WSH 03	239.269	
	WSH 04	240.759	
2	WSH 05	239.338	239.819
	WSH 06	239.228	
	WSH 07	239.952	
	WSH 08	239.294	239.340
3	WSH 09	239.385	
	<b>Total Average Reduced Level</b>		<b>239.433m</b>

This zonal averaging approach reduces vertical bias, particularly in shallow or vegetation-obstructed sections of the reservoir. While the current methodology establishes a reliable baseline, future surveys could benefit from Differential GNSS combined with geoid modeling to derive orthometric heights directly at each sounding position.

Riverbed elevations were then computed by subtracting the measured depths from the zonal ARLWS values (Table 3), as expressed in Equation 3:

$$RL_{bed,j} = ARLWS_i - D_j \quad (3)$$

$j$  = sounding index

$i$  = zone that sounding  $j$  belongs to

$ARLWS_i$  = Average Reduced Water-Surface Level of the zone  $i$  that sounding  $j$  belongs to

$D_j$  = Measured depth at sounding  $j$

$RL_{bed,j}$  = Reduced level of the riverbed at sounding  $j$

Because all depth measurements were referenced to a benchmark-controlled height framework, the resulting RLs form a consistent baseline for future sedimentation assessments. Repeating this procedure in subsequent years will allow cut-and-fill analyses to quantify sediment deposition and erosion over time. Although the present study was conducted in a non-tidal environment, the following formulation is included solely to demonstrate how the workflow may be extended to tidal waterbodies. Under normal tidal conditions, the variation of the water surface elevation may be approximated as simple harmonic motion. Accordingly, the reduced level of the water surface at the time of sounding can be estimated using Equation (4), after which the measured depth is subtracted to obtain the reduced level of the riverbed.

When time is referenced from the occurrence of high water, the water surface elevation is given by:

$$H = h + r \cos \omega t = h + r \cos(180^\circ \times \frac{t}{T}) \quad (4)$$

However, where the time reference is taken from low water, which is common in field observations, Equation (4) is modified to Equation (5):

$$H = h - r \cos \omega t = h - r \cos(180^\circ \times \frac{t}{T}) \quad (5)$$

$H$  = Reduced level of the water surface at the time of sounding,

$h$  = Reduced level at Mean tide level,

$r$  = Semi-tidal range,

$T$  = Time interval between High water and Low water,

$t$  = Time interval between the sounding and the reference tidal extremum (high or low water)

$D$  = Measured depth.

The reduced level of the riverbed is then obtained as illustrated in Equation (3). For example, a bathymetric measurement taken at 10:35 hours recorded a depth of 10.5 m, with low and high water occurring at 08:35 and 14:55 hours, respectively, and corresponding reduced water surface levels of 38.920 m and 42.120m.

Reduced level of the water surface at high tide = 42.120m

Reduced level of the water surface at low tide = 38.920m

The Reduced level at Mean tide level ( $h$ ) =  $\frac{1}{2}(42.120 + 38.920) = 40.52m$

Semi tidal range ( $r$ ) =  $\frac{1}{2}(42.120 - 38.92) = 1.60m$

Time interval between High water and Low water ( $T$ ) = 6.33 hours

Time interval from the sounding period to low tide occurrence ( $t$ ) = 2 hours.

Reduced level at the water surface ( $H$ ) =  $h - r \cos \omega t = h - r \cos(180^\circ \times \frac{t}{T})$

Reduced level at the water surface ( $H$ ) = 39.65m

Reduced level at the sounded depth = 39.65m - 10.5m

Reduced level at the sounded depth = 29.15m

Equations (4 and 5) must be incorporated when working with tidal waterbodies, as converting depth measurements to reduced levels is critical not only for sedimentation analysis but also for integrating topographic and bathymetric datasets, supporting flood management, and guiding engineering applications. Relying solely on volume differences between successive surveys to estimate sediment deposition can be misleading, as water volume may change due to seasonal inflows, evaporation, or human withdrawals, and without a consistent water-level reference, volume-based comparisons cannot reliably indicate sediment accumulation. The validity of using volume changes depends on having water-level information for both datasets, and even then, the approach is limited by the assumption of a uniform water surface elevation across the entire reservoir for each survey period. Figure 3 summarises the complete workflow adopted in this study, from benchmark establishment and water-surface height transfer through

depth acquisition, depth-to-elevation conversion, and uncertainty assessment. Each stage is designed to ensure geodetic consistency of the derived bathymetric surface and its suitability as a baseline for future sedimentation analysis.

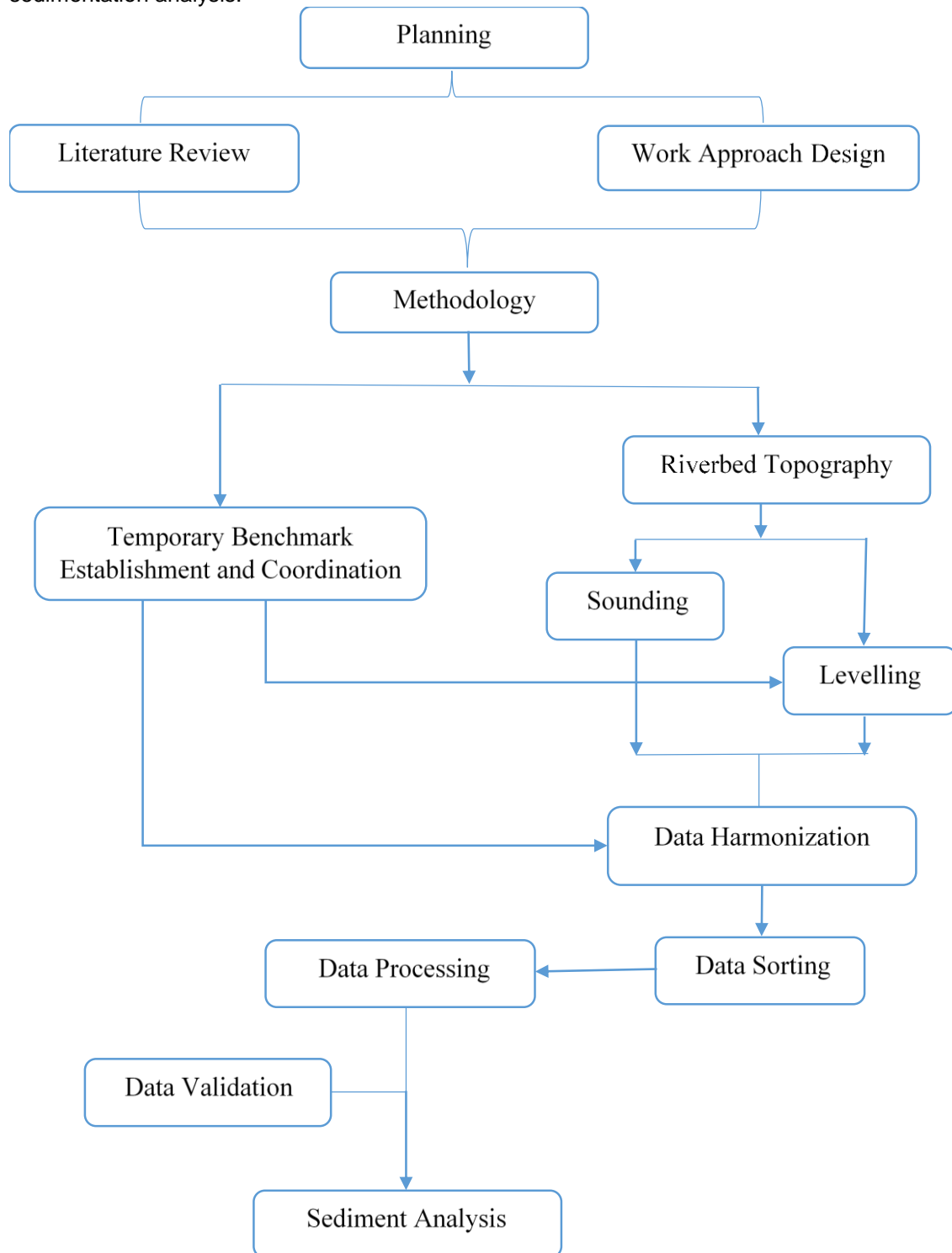


Figure 3: Workflow for depth-to-elevation conversion and riverbed elevation derivation

#### 4. RESULTS

The results presented in this section describe the benchmark-referenced riverbed elevations and associated measurement uncertainty derived from the survey and do not represent measured sediment thickness or sedimentation rates.

The final riverbed elevations for each zone, as summarized in Table 3, were computed using zonal average water-surface levels referenced to temporary benchmarks. This approach ensures accurate spatial representation of the riverbed and provides essential baseline data for assessing future sediment deposition in the reservoir.

Positioning accuracy was evaluated using repeat GNSS observations at established benchmarks. Vertical uncertainty was estimated through error propagation incorporating four independent components: GNSS positioning error, levelling closure error, transducer draft tolerance, and single-beam depth measurement precision. The combined vertical uncertainty ( $U_x$ ) was computed using Equation 6:

$$U_x = \sqrt{\sigma_{GNSS}^2 + \sigma_{LEVEL}^2 + \sigma_{DRAFT}^2 + \sigma_{ECHO}^2} \quad (6)$$

Where  $\sigma_{GNSS}^2$  represents the GNSS positioning uncertainty,  $\sigma_{LEVEL}^2$  the levelling closure error,  $\sigma_{DRAFT}^2$  the instrument draft tolerance, and  $\sigma_{ECHO}^2$  the depth measurement precision of the Echosounder.

Accordingly, only elevation changes exceeding the combined vertical uncertainty threshold can be interpreted as meaningful bed-level variation in future repeat surveys. Using representative survey values, Equation (6) becomes:

$$U_x = \sqrt{0.02^2 + 0.09^2 + 0.04^2 + 0.06^2}$$

$$U_x = 0.117 \text{ m} (\approx 0.12 \text{ m})$$

This result illustrates how the procedure quantifies uncertainty and defines a practical detection threshold for depth change analysis. In this example, depth variations smaller than approximately 0.12 m would fall within the measurement uncertainty range and would not be interpreted as meaningful elevation change. Validation of the workflow can be performed, where required, using independent measurements such as manual lead-line checks and RMSE comparison; however, the primary intent of the method is to provide a structured framework that can be adapted to different instruments, field conditions, and survey environments.

The purpose of this calculation is to demonstrate the application of the uncertainty framework rather than prescribe a fixed performance value, enabling future users to substitute their own equipment- and site-specific parameters.

Table 3: Extract of Riverbed Elevations by Zone

ZONE	ID	Easting (m)	Northing (m)	Depth (m)	Average Reduced Level of Water Surface (m)	Reduced Level of the Riverbed (m)
1	1	598741.672	871654.347	2.9	239.140	236.24
	2	598569.349	871549.796	1.3		237.84
	3	598698.381	871588.184	3.5		235.64
	4	598972.795	871805.442	4.6		234.54
	5	598517.937	871413.391	5.6		233.54
	6	598965.438	871895.283	1.4		237.74
	7	598431.334	871281.082	3.6		235.54
	8	598713.097	871408.579	3.8		235.34
	9	598564.451	871354.594	5.6		233.54
	10	598447.668	871421.563	4.4		234.74
2	1	599442.392	872017.846	2.9	239.819	236.92
	2	599806.641	872242.427	3.4		236.42

3	599582.069	871841.482	1.6		238.22
4	599385.218	872291.413	1.0		238.82
5	599536.319	872060.289	2.3		237.52
6	599847.467	872593.617	4.4		235.42
7	599519.982	871919.867	1.5		238.32
8	599215.356	871901.821	3.0		236.82
9	599461.994	872033.328	2.8		237.02
10	599751.927	872230.983	3.2		236.62
<b>3</b>	<b>1</b>	<b>600183.941</b>	<b>872732.469</b>	<b>1.0</b>	<b>239.340</b>
	2	600004.268	872717.752	3.6	235.74
	3	600145.547	872861.593	2.6	236.74
	4	600294.184	872915.417	2.7	236.64
	5	600105.536	872670.392	0.9	238.44
	6	600031.214	872643.438	2.0	237.34
	7	600047.549	872783.917	2.7	236.64
	8	600231.374	872833.748	2.6	236.74
	9	599981.397	872827.194	1.2	238.14
	10	600015.789	872663.036	3.4	235.94

The calculated riverbed elevations can be used to estimate sediment thickness at different levels, especially when compared with data from future surveys. This method is most effective in soft ("fluff") areas of the riverbed. For distinguishing between hard and soft layers, a Dual-Frequency Echosounder is recommended. Alternatively, a Multibeam Echosounder or Sub-Bottom Profiler can be employed for higher-resolution mapping and subsurface layer visualization. Nevertheless, this workflow is suitable for monitoring sediment deposits in newly constructed reservoirs. When sediment levels are measured between hard and soft layers using a Leadline, this method can also provide useful complementary data.

Table 4 presents scenario-based volume estimates generated by incrementally raising the mapped riverbed surface derived from field-measured bathymetric data. These values do not represent observed sediment accumulation or measured sediment thickness at the time of survey. Rather, they demonstrate how the benchmark-referenced bathymetric surface produced by this methodology can be used as a baseline for evaluating potential capacity displacement under assumed vertical infilling conditions in future assessments.

Table 4. Hypothetical capacity displacement under assumed uniform vertical infilling

Proposed sediment levels	Volume of the Earthwork (m <sup>3</sup> )	Default Earthwork Volume (m <sup>3</sup> )	Sediment thickness Volume (m <sup>3</sup> )
<b>+1m</b>	181,742,432.884		771,615.927
<b>+2m</b>	180,970,816.957		1,543,231.854
<b>+3m</b>	180,199,201.030		2,314,847.781
<b>+4m</b>	179,427,585.103	182,514,048.811	3,086,463.708
<b>+5m</b>	178,655,969.175		3,858,079.636
<b>+6m</b>	177,884,353.248		4,629,695.563

While Table 4 presents the baseline sediment volumes above the soft riverbed layer, future assessments will require comparing riverbed elevations from successive surveys. By generating and contrasting Digital

Elevation Models (DEMs) over time, areas of sediment deposition and erosion can be identified, and their respective volumes accurately quantified.

## 5. DISCUSSIONS

The volume estimates presented herein are scenario-based analyses derived from hypothetical vertical displacement of the mapped riverbed surface and are intended solely to illustrate reservoir capacity sensitivity. They do not represent observed sediment accumulation or temporal sedimentation trends. Analysis of Table 5 illustrates the theoretical relationship between incremental vertical infilling of the reservoir bed and corresponding reductions in available storage volume, assuming a uniform upward displacement of the mapped riverbed surface. The results are intended to demonstrate the sensitivity of reservoir capacity to relatively small vertical changes in bed elevation, particularly in shallow systems. These scenarios do not imply that such infilling has occurred or will occur over a specific time frame; rather, they serve as a methodological illustration of how the derived bathymetric surface can be applied in capacity-loss analysis once repeat surveys or independent sediment thickness measurements become available.

Table 5. Hypothetical reservoir capacity response to assumed bed-elevation rise

Sediment Level	Sediment Volume (m <sup>3</sup> , Independent)	Volume of the Reservoir (m <sup>3</sup> )	Volume Left (m <sup>3</sup> )	Percentage Loss (%)	Remarks
+1m	771,615.927		1,486,022.980	34.178	
+2m	1,543,231.854		714,407.053	68.356	
+3m	2,314,847.781		LAND	> 100 (102.544)	The reservoir is mostly filled; water is only in the sediment pores
		2,257,638.907m <sup>3</sup>			
+4m	3,086,463.708		LAND	—	Filled up
+5m	3,858,079.636		LAND	—	Filled up
+6m	4,629,695.563		LAND	—	Filled up

Figure 4 visually represents the data in Table 5, facilitating understanding for non-specialists and allowing easy reference by various agencies when required.

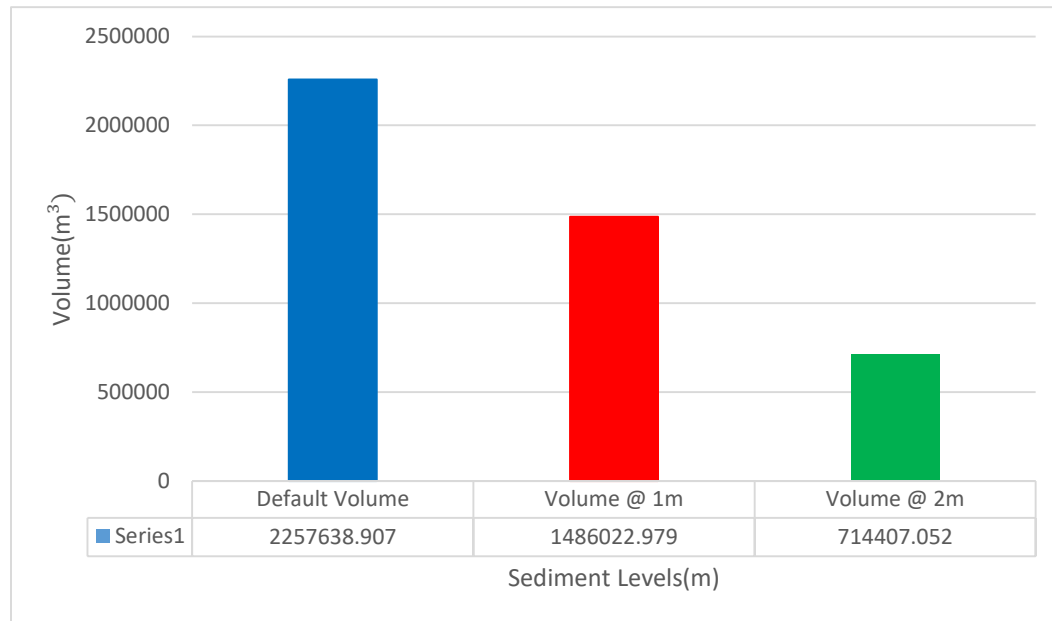


Figure 4: Hypothetical effect of uniform bed infilling on reservoir storage volume

The majority of depth readings in the reservoir are between 1 and 3 meters (Figure 5), with fewer readings in the 4 to 6 meter range. Even modest vertical infilling of the Erelu Reservoir bed can substantially reduce storage capacity. Scenario-based analysis indicates that a 1 m rise would cause a 34.18 % loss, while 2 m of accumulation would result in a 68.36 % reduction, potentially leading to full siltation at higher levels. Full siltation is projected between 3–6 m of sediment accumulation because the reservoir's shallow geometry and limited storage volume cause the mapped bed elevation to approach the water surface, leaving little or no remaining storage. These results have direct implications for sediment management: regular monitoring can detect early-stage deposition, guiding dredging schedules to prevent critical capacity loss. Furthermore, the zonal benchmark-referenced workflow enables precise identification of localized sediment hotspots, supporting targeted interventions rather than blanket dredging. Adopting such strategies helps sustain water availability, prolong reservoir lifespan, and informs upstream erosion control and sediment mitigation planning.

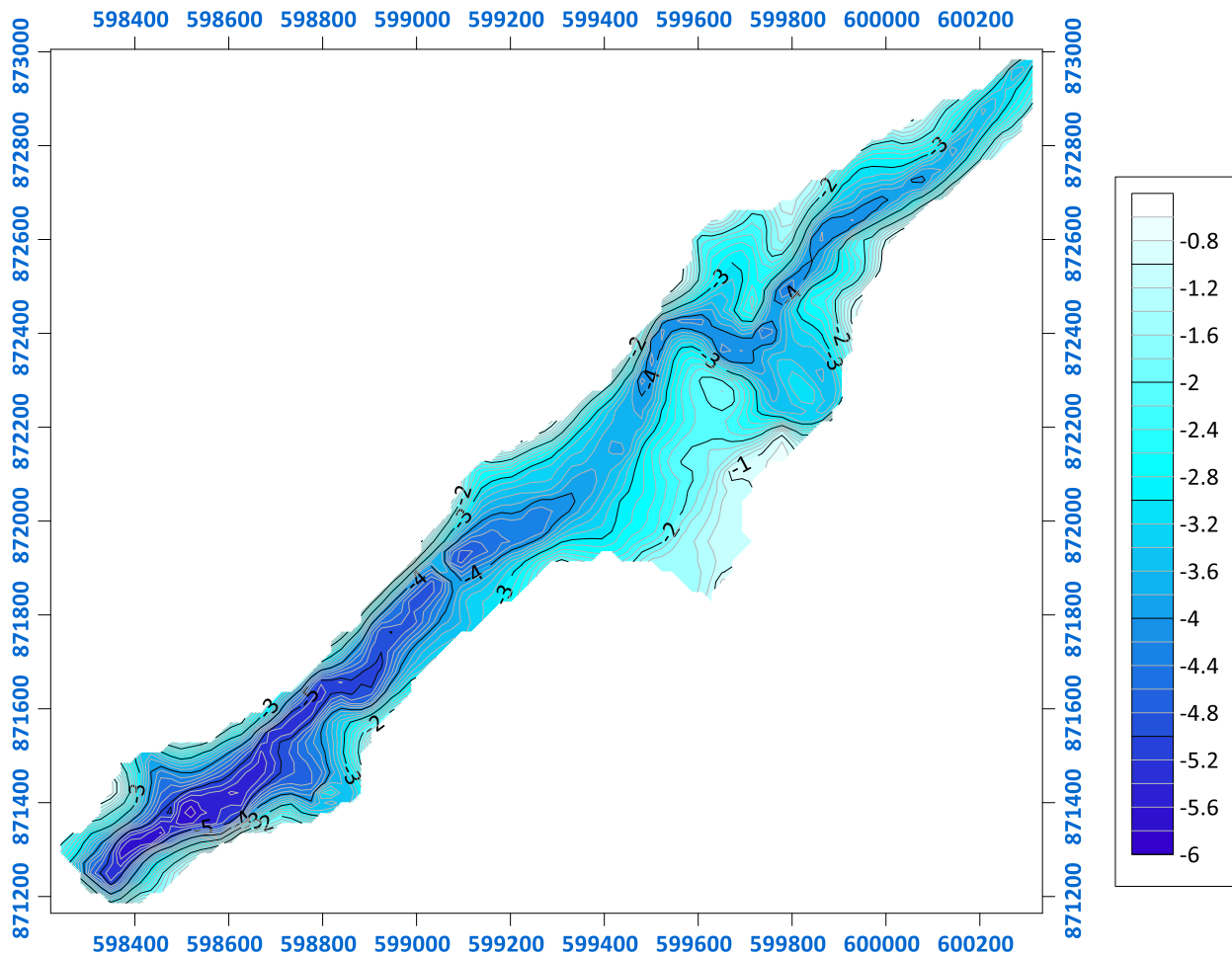


Figure 5. Distribution of measured reservoir depths, mostly between 1–3 m.

## 6. CONCLUSION

This study presents a benchmark-controlled, GNSS-integrated single-beam bathymetric workflow for converting depth measurements into geodetically referenced riverbed elevations in shallow reservoirs. Scenario analysis demonstrates that, if future surveys detect uniform bed-elevation increases of 1–2 m, substantial reductions in storage capacity would theoretically occur, emphasizing the importance of accurate baseline establishment and periodic monitoring. Temporary control points were established along the riverbank, and orthometric heights were precisely transferred to the water surface to ensure high positional accuracy. Dividing the Erelu Reservoir into distinct zones with assigned average water surface elevations enhanced the precision of depth-to-height conversion and minimized potential errors. The results revealed significant volume loss at sediment depths of 1–2 m and potential full infilling beyond 3 m,

suggesting that, should future surveys confirm comparable vertical bed-elevation increases, dredging may be required to preserve storage capacity and support sediment management. While the method provides a valuable baseline for monitoring sedimentation and managing local contaminants, it is limited in differentiating sediment layers. Future studies are encouraged to integrate dual-frequency Echosounders and GNSS-based geoidal referencing for improved layer resolution. These findings support informed decision-making in reservoir maintenance by emphasizing timely sediment removal, storage capacity restoration, and enforcement of upstream land-use and erosion control measures to reduce sediment inflow. Overall, the methodology offers a replicable approach for generating baseline bathymetric data in shallow or newly formed waterbodies, providing a foundation for future sedimentation monitoring and integrated watershed management. All procedures adhered strictly to SURCON and IHO standards, affirming the method's reliability for reservoir monitoring.

## ACKNOWLEDGEMENTS

The authors sincerely appreciate the various data sources used in this study and the technical support provided by relevant institutions. We are also grateful for the valuable input from experts and colleagues who contributed to improving the manuscript. The constructive feedback from the editor, reviewers, respondents, and other anonymous contributors is deeply acknowledged and appreciated.

## REFERENCES

Abdullah, M. I. C., Sah, A. S. R. M., & Haris, H. (2020). Geoaccumulation index and enrichment factor of arsenic in surface sediment of Bukit Merah Reservoir, Malaysia. *Tropical Life Sciences Research*, 31(3), 109–125.

Adediji, A. (2005). Reservoir sedimentation: The case of the Opa Reservoir catchment, southwestern Nigeria. *South African Geographical Journal*, 87(2), 123–128.

Adongo, T. A., Kyei-Baffour, N., Abagale, F. K., & Agyare, W. A. (2020). Assessment of reservoir sedimentation of irrigation dams in northern Ghana. *Lake and Reservoir Management*, 36(1), 87–105.

Ajith, A. V. (2016). Bathymetric survey to study the sediment deposit in the reservoir of Peechi Dam. *IOSR Journal of Mechanical and Civil Engineering*, 3(1), 34–38.

Castillo, L. G., Carrillo, J. M., & Álvarez, M. A. (2015). Complementary methods for determining the sedimentation and flushing in a reservoir. *Journal of Hydraulic Engineering*, 141(11), 05015004.

Ceylan, A., Karabork, H., & Ekozoglu, I. (2011). An analysis of bathymetric changes in Altınapa Reservoir. *Carpathian Journal of Earth and Environmental Sciences*, 6(2), 15–24.

Chukwu Fidelis, N., & Badejo, O. T. (2015). Bathymetric survey investigation of Lagos Lagoon seabed topographical changes. *Journal of Geosciences and Geomatics*, 3(2), 37–43.

Dadoria, D., Tiwari, H. L., & Jaiswal, R. K. (2017). Assessment of reservoir sedimentation in Chhattisgarh State using remote sensing and GIS. *International Journal of Civil Engineering and Technology*, 8(4), 526–534.

Darama, Y., Selek, Z., Selek, B., Akgul, M. A., & Dagdeviren, M. (2019). Determination of sediment deposition of Hasanlar Dam using bathymetric and remote sensing studies. *Natural Hazards*, 97(1), 211–227.

Essel-Yorke, K. A., Anim, M., & Nyarko, B. K. (2023). Sedimentation assessment using hydrological simulation and bathymetry survey: The case of River Amissa drainage basin, Ghana. *Heliyon*, 9(3).

Falaye, A. E., Ajani, E. K., Kareem, O. K., & Olanrewaju, A. N. (2015). Assessment of ichthyofaunal assemblage of Erelu Reservoir, Oyo, Nigeria. *Ecologia*, 5(2), 43–53.

Güvel, Ş. P., Akgül, M. A., & Yurtal, R. (2021). Investigation of sediment accumulation in Berdan Dam Reservoir using bathymetric measurements and Sentinel-2 data. *Arabian Journal of Geosciences*, 14(24), 2723.

Iqlash, S. M., Arunbabu, E., Wahid, A. A., et al. (2025). Reservoir capacity and sedimentation assessment by integrating echo sounding and remote sensing techniques. *Journal of the Indian Society of Remote Sensing*, 53, 1311–1323.

Jothiprakash, V., & Garg, V. (2009). Reservoir sedimentation estimation using artificial neural networks. *Journal of Hydrologic Engineering*, 14(9), 1035–1040.

Kareem, O. K., Ajani, E. K., Omitoyin, B. O., Olanrewaju, A. N., Orisasona, O., & Osho, E. F. (2018). Spatial and temporal limnological status of Erelu Reservoir, southwestern Nigeria. *Ife Journal of Science*, 20(3), 509–518.

Lopes, J. W. B., & de Araújo, J. C. (2019). Simplified method for the assessment of siltation in semiarid reservoirs using satellite imagery. *Water*, 11(5), 998.

Mekonnen, Y. A., Mengistu, T. D., Asitatikie, A. N., & Kumilachew, Y. W. (2022). Evaluation of reservoir sedimentation using bathymetry survey: A case study on Adebra night storage reservoir, Ethiopia. *Applied Water Science*, 12(12), 269.

Mohammad, M. E., Al-Ansari, N., & Knutsson, S. (2016). Annual runoff and sediment in Duhok Reservoir watershed using SWAT and WEPP models. *Engineering*, 8(7), 410–422.

Moningkey, A. T., Rampengan, M. M. F., Tumengkol, A. A., & Kumaat, J. C. (2022). Study of bathymetry and sedimentation in Tondano Lake. In *IOP Conference Series: Earth and Environmental Science* (Vol. 986, No. 1, Article 012038). Bristol, England: IOP Publishing.

Mostofi, K. H., Hossein, M. O., Bayat, S. H., Khiali, G. V., & Adineh, M. (2019). River sediment monitoring using remote sensing and GIS. *IOSR Journal of Engineering*, 9(3), 23–30.

Olasunkanmi, N. K., Sunmonu, L. A., Owolabi, D. T., Bawallah, M., & Oyelami, A. (2021). Investigation of dam integrity from electrical resistivity methods: A case of Erelu Dam, southwestern Nigeria. *Indonesian Journal on Geoscience*, 8(2), 265–274.

Ortt, R. A., VanRyswick, S., & Wells, D. (2007). Bathymetry and sediment accumulation of Triadelphia and Rocky Gorge reservoirs. Maryland Dept of Natural Resources, Maryland Geological Survey, Coastal and Estuarine Geology, Baltimore.

Patil, R., & Shetkar, R. (2015). Sediment deposition in Koyna Reservoir by integrated bathymetric survey. *International Journal of Research in Engineering and Technology*, 4(11), 114–118.

Patil, R., & Shetkar, R. (2016). Prediction of sediment deposition in reservoirs using analytical methods. *American Journal of Civil Engineering*, 4(6), 290–297.

Patro, E. R., De Michele, C., Granata, G., & Biagini, C. (2022). Assessment of current reservoir sedimentation rate and storage capacity loss: An Italian overview. *Journal of Environmental Management*, 320, 115826.

Popoola, K., Sowunmi, A., & Amusat, A. (2019). Comparative study of physicochemical parameters with national and international standards and insect community of Erelu Reservoir in Oyo State, Nigeria. *International Journal of Water Resources and Environmental Engineering*, 11(3), 56–65.

Shiferaw, M., & Abebe, R. (2021). Reservoir sedimentation and estimating dam storage capacity using bathymetry survey: A case study of Abrajit Dam, Upper Blue Nile Basin, Ethiopia. *Applied Geomatics*, 13(3), 277–286.

Shittu, I. O., Olorunkosebi, H. O., Hamid-Mosaku, A. I., Jimoh, O. A., Akindiya, O. M., Oyelakin, L. O., Muhammed, L. O., & Raheem, K. A. (2024). An efficient bathymetric assessment of Erelu Reservoir for its sustainability. *Uniport Journal of Engineering and Scientific Research*, 8(2), 101–120.

Singh, S., Prasad, B., & Tiwari, H. L. (2023). Sedimentation analysis for a reservoir using remote sensing and GIS techniques. *ISH Journal of Hydraulic Engineering*, 29(1), 71–79.

Springs, L. C. (2008). *Volumetric and sedimentation survey of Lake Cypress Springs* (Technical report). Austin, TX: Texas Water Development Board.

Ufoegbune, G., Ladipo-Ajai, O., Oyedepo, J., & Eruola, A. (2009). GIS application to municipal water supply planning in Abeokuta Metropolis, southwestern Nigeria. *Journal of Meteorology and Climate Science*, 7, 23–27.